

# Geophysical Research Letters



## RESEARCH LETTER

10.1029/2019GL083273

### Key Points:

- The depth-averaged temperature more realistically characterizes ocean response than pre-TC sea surface temperature
- The parameterization of the air-sea exchange process is important in computing the thermodynamic energy budget for TCs
- A revised predictor including two key factors shows significant improvement in the TC intensity change prediction

### Supporting Information:

- Supporting Information S1

### Correspondence to:

S.-H. Kim,  
yah13@hanmail.net

### Citation:

Lee, W., Kim, S.-H., Chu, P.-S., Moon, I.-J., & Soloviev, A. V. (2019). An index to better estimate tropical cyclone intensity change in the western North Pacific. *Geophysical Research Letters*, 46, 8960–8968. <https://doi.org/10.1029/2019GL083273>

Received 16 APR 2019

Accepted 8 JUL 2019

Accepted article online 16 JUL 2019

Published online 14 AUG 2019

©2019. The Authors.

This is an open access article under the terms of the Creative Commons Attribution-NonCommercial-NoDerivs License, which permits use and distribution in any medium, provided the original work is properly cited, the use is non-commercial and no modifications or adaptations are made.

## An Index to Better Estimate Tropical Cyclone Intensity Change in the Western North Pacific

Woojeong Lee<sup>1</sup>, Sung-Hun Kim<sup>2,3</sup> , Pao-Shin Chu<sup>3</sup>, Il-Ju Moon<sup>2</sup> , and Alexander V. Soloviev<sup>4</sup>

<sup>1</sup>National Typhoon Center, Korea Meteorological Administration, Jeju, Republic of Korea, <sup>2</sup>Graduate Program in Marine Meteorology/Typhoon Research Center, Jeju National University, Jeju, Republic of Korea, <sup>3</sup>Department of Atmospheric Sciences, School of Ocean and Earth Science and Technology, University of Hawai'i at Mānoa, Honolulu, HI, USA, <sup>4</sup>Halmos College of Natural Sciences and Oceanography, Nova Southeastern University, Dania Beach, FL, USA

**Abstract** A revised predictor called the net energy gain rate (*NGR*) is suggested by considering wind-dependent drag coefficient based on the existing maximum potential intensity theory. A series of wind speed-dependent *NGR*, known as *NGR-w*, is calculated based on pretropical cyclone (TC) averaged ocean temperatures from the surface down to 120 m (at 10-m intervals) to include the TC-induced vertical mixing for 13 years (2004–2016) in the western North Pacific. It turns out that *NGR*<sub>50-w</sub> (*NGR-w* based on temperature averaged over top 50 m) has the highest correlation with 24-hr TC intensity change compared with the commonly used sea surface temperature-based intensification potential (*POT*), depth-averaged temperature-based *POT* (*POT*<sub>DAT</sub>), and constant drag coefficient in the *NGR*. To demonstrate the effectiveness of *NGR*<sub>50-w</sub>, we designed and conducted experiments for training (2004–2014) and testing (2015–2016). The model with *NGR*<sub>50-w</sub> shows greater skill than does the model with *POT*<sub>DAT</sub> or *POT* by reducing prediction errors by about 16%.

## 1. Introduction

While track prediction of tropical cyclones (TCs) has improved steadily over the last three decades (Rappaport et al., 2012), there has been comparatively little advancement in intensity prediction due to the complicated physical mechanisms involved in internal TC dynamics and their interaction with upper ocean and atmospheric circulation (Elsberry et al., 2013). It is of utmost importance to accurately predict the rapid intensifying and weakening of TCs at the shorter range (within 24 hr) because landfalling TCs can undergo significant and quick intensity changes, which could cause huge economic losses and casualties (Lin et al., 2009). Moreover, landfalling typhoons over the East Asian coast, including China, Japan, Korea, and Taiwan, have shown increased intensity since the late 1970s (Mei & Xie, 2016). Improving rapid intensification forecasts is one of the highest priorities for TC forecasters among many nations and a central focus area of the National Oceanic and Atmospheric Administration's Hurricane Forecast Improvement Project (Gall et al., 2013).

Numerous attempts have been made to predict the 24-hr intensity change, especially for the rapid intensification cases, based on a statistical-dynamical model (DeMaria et al., 2012; Gao et al., 2016; Kaplan et al., 2010; Rozoff & Kossin, 2011) as well as numerical modeling perspectives (Chen & Gopalakrishnan, 2014; Tallarpragada & Kieu, 2014). According to recent studies, the statistical-dynamical model still shows more skill at all forecast times compared to dynamical models (DeMaria et al., 2014; Kim et al., 2018). Much effort has gone into improving the TC intensity forecast using new predictors (Kaplan et al., 2015), optimizing predictors (Balaguru et al., 2018; Goni et al., 2009; Rozoff & Kossin, 2011), or applying a nonlinear approach (Lin et al., 2017) instead of using the multiple linear regression method. In other words, finding and utilizing a new predictor that accurately represents TC intensity change holds promise for improving forecast performance in statistical-dynamical models.

In exploring the ocean's role in TC intensity changes, it is important to understand the upper ocean thermal structure because of its interaction with TCs (Emanuel et al., 2004; Goni et al., 2009; Kaplan et al., 2010; Lin et al., 2008; Pun et al., 2007; Shay et al., 2000; Wada & Usui, 2007). To estimate the ocean thermal field accounting for the sea surface cooling effect by TC-induced vertical mixing, Price (2009) suggested the depth-averaged temperature (*DAT*),

$$DAT_d = \frac{1}{d} \int_{-d}^0 T dz, \quad (1)$$

where  $d$  is the depth of vertical mixing induced by TCs.  $DAT$  is a more direct and robust metric of the ocean thermal field reflecting interaction between TCs and the ocean than the widely used tropical cyclone heat potential, because the latter may misrepresent oceanic conditions in shallow waters.

Maximum potential intensity ( $MPI$ ) is widely used to estimate the maximum surface wind speed given atmospheric and oceanic environment (Emanuel, 1988, 1995). Lin et al. (2013) modified  $MPI$ , which is determined by the thermodynamic conditions of sea surface temperature ( $SST$ ) and the atmospheric environment for steady state TCs (Emanuel, 1988; Holland, 1997), and used  $DAT$  to form a new ocean coupling potential intensity ( $OC\_PI$ ) index

$$OC\_PI^2 = \frac{DAT - T_0}{T_0} \frac{C_k}{C_d} (k^* - k), \quad (2)$$

where  $T_0$  is the TC outflow temperature determined by the atmospheric vertical profile,  $C_k$  is the enthalpy exchange coefficient,  $C_d$  is the drag coefficient,  $k^*$  is the saturation enthalpy of the sea surface, and  $k$  is the surface enthalpy in the TC environment. It has been shown that  $OC\_PI$  reduces overestimation of maximum intensity relative to  $SST$ -based  $MPI$  (Lin et al., 2013). In recent years,  $OC\_PI$  has been frequently used to predict intensity and rapid intensification (Balaguru et al., 2015; Gao et al., 2016).

The air-sea exchange processes control the evolution of TCs (Emanuel, 2003). The TC intensity depends on the coefficients of the transfers of momentum ( $C_d$ ) and enthalpy ( $C_k$ ) between the ocean and the atmospheric boundary layer (Emanuel, 1986; Ooyama, 1969). The effects of wind speed-dependent exchange coefficients on TCs have been demonstrated in several previous studies (Braun & Tao, 2000; Bao et al., 2012; Green & Zhang, 2013; Jenkins, 2002; Moon et al., 2007; Nolan, Zhang, et al., 2009; Nolan, Stern, et al., 2009), and the parameterizations of  $C_d$  were deemed a key determinant of TC intensity simulation. The general consensus is that the  $C_d$  increases with wind speed until it reaches approximately 60 kt and does not increase above 70 kt (Bell et al., 2012; Donelan et al., 2004; Jarosz et al., 2007; Powell et al., 2003). However, there are still conflicting results and unresolved issues concerning  $C_d$  at very high wind speeds above 120 kt due to limited observations and experiments (Bell et al., 2012; Montgomery et al., 2010; Rotunno & Emanuel, 1987). At extremely high wind speeds above approximately 120 kt, Soloviev et al. (2014) showed that the  $C_d$  increases using the unified waveform and two-phase parameterization schemes, whereas Takagaki et al. (2012) showed the value of  $C_d$  approaches to constant based on their laboratory measurements. A proper value of  $C_d$  at high wind speeds is important to know because the incidence of categories 4 and 5 storms in the northwest Pacific have increased over the last 37 years (Mei & Xie, 2016).

The objective of this study is to improve intensity prediction, especially in a short temporal range of 24 hr. We develop a synoptic predictor for intensity change, a net energy gain rate ( $NGR$ ), which is based on the  $MPI$  theory (Emanuel, 1988). This predictor is derived from  $DAT$  and a new parameterization scheme of  $C_d$  depending on wind speed. A verification of  $NGR$  is conducted using a perfect prognosis-based multiple linear regression model for the training and test period. The data and methodology are described in section 2. Section 3 presents an improvement in  $NGR$  for TC intensity change. Section 4 compares  $NGR$  with two other comparable new indices suggested by others. Discussion and conclusion are given in section 5.

## 2. Data and Methodology

### 2.1. TC Best Track, Atmospheric, and Oceanic Data

In this study, TC statistics over the western North Pacific during 2004–2016 are obtained from the best track data archived by the Joint Typhoon Warning Center (JTWC). Statistics for analysis are calculated only for TCs that had a wind speed at or above 34 kt. The  $SST$  and  $DAT$  were calculated using the Hybrid Coordinate Ocean Model (HyCOM) Navy Coupled Ocean Data Assimilation (NCODA) nowcast/forecast system data provided by the Naval Research Laboratory. These oceanic variables were averaged within a radius of 200 km from the storm center using prestorm conditions (3 days before). The  $DAT$  was calculated at various  $d$  (10–120 m, at 10-m interval;  $DAT_{10}$ – $DAT_{120}$ ) and used to calculate the ocean component of  $OC\_PI$  ( $OC = PI_{10}$ – $OC = PI_{120}$ ; hereafter named  $OC\_PIs$ ). The  $OC\_PIs$  are calculated based on Emanuel's

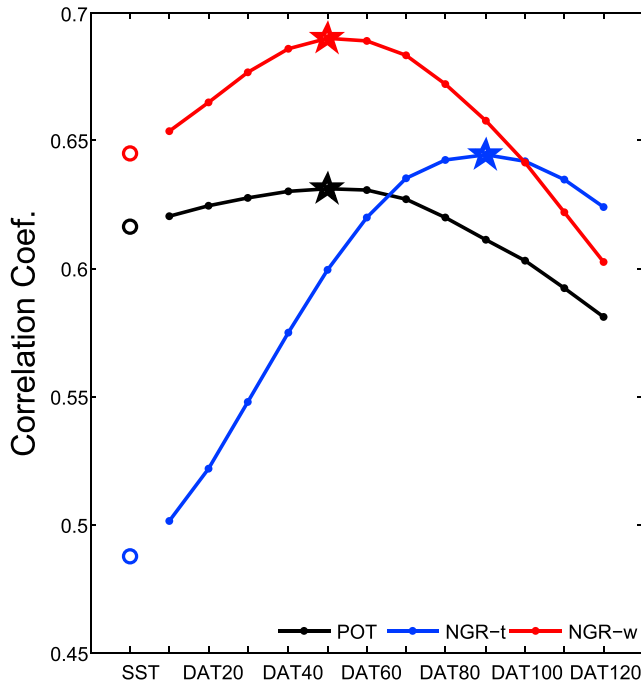


**Figure 1.** The comparison of the correlation coefficients between a series of *POT*, *NGR-t*, and *NGR-w* from *SST* to *DAT*<sub>120</sub> by computed ocean temperature averaged over surface to 120-m depth (at 10-m interval) and the 24-hr changes in TC intensity during 2004–2016. Pentagrams represent the location of the maximum value for each group. *POT* = the intensification potential; *NGR-t* = net energy gain rate using constant drag coefficient; *NGR-w* = same as *NGR-t* but for changing drag coefficient.

( $G_{DAT}$ ) and wind-dependent  $C_d$ -based  $D$  ( $D_w$ ) at the “current intensity” resulting from the given thermodynamic environment.

$$NGR = G_{DAT} - D_w = \frac{DAT - T_0}{T_0} C_k \rho V_s (k_0^* - k) - C_{d(V_s)} \rho V_s^3 \quad (6)$$

Larger (smaller) *NGR* implies that the more (less) energy will be used for TC intensification. Note that while *NGR* is the difference between  $G$  and  $D$  at the current intensity, when  $G = D$  and therefore  $NGR = 0$ , the TC reaches a steady state and *MPI* can be derived by solving for  $V_s$ . The *NGR* was computed and formulated in two ways to conduct a sensitivity test to evaluate the impact of  $C_d$  dependence on wind speed for parameterization of the air-sea exchange process. The first one is a default where  $C_d$  is set to be a constant ( $1.33 \times 10^{-3}$ ) in equation (6) using the *pcmin.m* program, hereafter referred to as the “traditional set of *NGR* (*NGR-t*).” The second is derived from equation (6), but  $C_d$  fitting depending on wind speed is applied instead of the traditionally used constant  $C_d$ . For winds below 120 kt, we utilize the unified  $C_d$  parameterization scheme interpolated from available field and laboratory data (Soloviev et al., 2014). For winds above 120 kt,  $C_d$  is assumed to be constant ( $2.0 \times 10^{-3}$ ). This will be referred to as the “wind dependency set of *NGR* (*NGR-w*).” The *MPI* is averaged along the track of the storm using the best track data positions at 6-hr intervals excluding current forecast time.

### 3. Results

The intensification potential (*POT*) is defined as the difference between *MPI* and the current intensity. The *POT* is considered the most important predictor in the statistical-dynamical TC intensity prediction models (Chen et al., 2011; DeMaria & Kaplan, 1994, 1999). In particular, *DAT*-based *POT* shows the highest correlation coefficient with intensity change (Kim et al., 2018). We note that like *POT*, our new predictor *NGR* is also related to the difference between *MPI* and current intensity, but the relationship takes a different functional form. Figure 1 presents the correlation coefficients between 24-hr TC intensity change and various

“*pcmin.m*” MATLAB function, which is available online (<ftp://texmex.mit.edu/pub/emanuel/TCMAX/pcmin.m>). Atmospheric variables were calculated using Global Forecasting System analysis data with  $1^\circ \times 1^\circ$  spatial and 6-hr temporal resolution provided by the National Centers for Environmental Prediction (NCEP).

#### 2.2. The New *NGR*

The energy cycle of a mature TC is one of isothermal expansion, adiabatic expansion, isothermal compression, and adiabatic compression (Bister & Emanuel, 1998). Based on Emanuel’s *MPI* theory, the energy generation rate ( $G$ ) into the TCs from the sea surface for each square meter of sea surface covered by the storm and the surface frictional dissipation rate ( $D$ ) in the system for each square meter of ocean are given by

$$G = \frac{T_s - T_0}{T_0} C_k \rho V_s (k^* - k), \quad (3)$$

$$D = C_d \rho V_s^3, \quad (4)$$

where  $C_k$  is constant value  $1.2 \times 10^{-4}$ ,  $T_s$  is *SST* and  $V_s$  is the surface wind speed. The *MPI* is reached at the wind speed where  $G$  becomes equal to  $D$ . Thus, setting  $G$  equal to  $D$  and solving for  $V_s$ , an expression for the maximum possible sustained surface wind speed of a TC is obtained.

$$MPI^2 = \frac{T_s - T_0}{T_0} \frac{C_k}{C_d} (k^* - k) \quad (5)$$

An *NGR* for the western North Pacific basin is developed by incorporating *OC-PI* and wind-dependent drag coefficient based on the *MPI* framework. The *NGR* expresses the realistic response of the sea surface cooling and wave states by TC defined as the difference between *DAT*-based  $G$

mixing depths for three groups—*POT*, *NGR-t*, and *NGR-w*—during 2004–2016. Note that the correlation is also carried out for *SST* alone, which is shown at the leftmost margin of the abscissa.

For each group, *DAT*-based variables generally exhibit higher correlation coefficients than do *SST*-based variables, which are denoted by an open circle in Figure 1, revealing the importance of using *DAT*. For example, for *SST*-based variables the correlation is 0.48, but it reaches as high as 0.64 at *DAT*<sub>90</sub> for *NGR-t* (blue curve). For shallow and moderate *DAT* ( $\leq 60$  m), *NGR-t* has lower correlations than has *POT*. The value of constant  $C_d$  (0.0013) used to calculate *NGR-t* is much lower than the observed  $C_d$  in the range from 35 to 63 kt, shown from previous studies, where probability density of observed TC intensity covers 47.7% of the total (not shown). When constant  $C_d$  is used, the  $D$  for *NGR-t* is underestimated, which results in lower correlation with 24-hr TC intensity change than *POT* for *DAT*  $\leq 60$  m. *DAT*-based *POT* (black curve) correlates significantly with the intensity change at the 1% test level as reported in a previous study (Kim et al., 2018). Note that an even higher correlation coefficient (0.69) is found between the TC intensity change and *DAT*-based *NGR-w* (red curve). This implies that the dependence of the wind speed on  $C_d$  in many studies is important because  $C_d$  plays an important role in contributing to the energy budget for TC intensity. Because *NGR-w* using a wind speed-dependent  $C_d$  represents the TC energy budget more realistically than does *NGR-t* using a traditional constant  $C_d$ , this new predictor is likely to exhibit the highest correlation to 24-hr TC intensity change.

It is somewhat surprising that the correlations between *NGR-w* and intensity change drop dramatically for *DAT*  $\geq 80$ . It is well known that the strength of maximum wind speed is the dominant factor in TC-induced vertical mixing, and the typical vertical mixing depth for a major TC (categories 3 to 5) is about 100 m (Price, 2009). The deep mixing depth ( $\geq 80$  m) based on *DAT* is suited for strong TCs but can cause underestimation of  $G$  in equation (3) for relatively weak TCs. Therefore, the correlation coefficient of deep *DAT*-based *NGR* is lower because the *DAT* used is too deep (or too cold) for weak TCs and the frequency of strong TC events is very low.

The correlation coefficient of *DAT*-based *POT* for the longer lead times after 42 hr tends to be higher than that of *NGR-w* (Figure S1). This is due to the use of the TC current intensity when  $G$  and  $D$  are calculated in equation (6). Consequently, the TC intensity uncertainty increases with increasing forecast lead time. According to Fisher's  $z$  test (Wilks, 2011), the difference in the correlation coefficient between *NGR-w* and other predictors is significantly different within 42-hr forecast lead times as denoted by the dashed lines in Figure S1 at the 5% test level (e.g., the  $p$  value is smaller than 0.05). Note that *DAT*-based *NGR-w* attains the maximum correlation coefficient with 24-hr TC intensity changes at 50 m (Figure 1). In Figure 2, we compare the spatial distribution of the composite of 24-hr observed TC intensity change, *NGR*<sub>50-w</sub>, *POT*, and *POT* at *DAT*<sub>50</sub> (*POT*<sub>50</sub>) for the period 2004–2016. The areas of observed positive TC intensity changes span the main TC development region (5–20°N, 110–160°E) in the warm pool of the Philippine Sea and the South China Sea before making landfall or undergoing extratropical transition (Figure 2a). The regions of negative TC intensity changes are found from the Yellow Sea extending northeastward through the Kuroshio extension region. *POT* and *POT*<sub>50</sub> have patterns similar to the observations but show TC intensity changes that are too strong throughout the main TC development region and too weak or rare at higher latitudes (Figures 2c and 2d). On the other hand, *NGR*<sub>50-w</sub> has a distribution closest to the observations in both positive and negative TC intensity change regions (Figure 2b). The pattern correlations between the observed 24-hr TC intensity change and the corresponding *POT*, *POT*<sub>50</sub>, and *NGR*<sub>50-w</sub> are computed over a 1° latitude-longitude box centered at each grid point for the period of 2004–2016. The correlations are 0.66, 0.68, and 0.77 for the aforementioned three predictors, respectively, and the correlation between *NGR*<sub>50-w</sub> and intensity change is statistically significant at the 1% level (Chu & Zhao, 2007) when Quenouille's (1952) method is used to account for the reduction in the effective number of degrees of freedom due to persistence. This result lends support that *NGR*<sub>50-w</sub>, which has the highest pattern correlation coefficient and captures most of the observations for a 24-hr TC intensity change. To compare the prediction skill of the main predictors (*POT*, *POT*<sub>50</sub>, *NGR*<sub>90-t</sub>, and *NGR*<sub>50-w</sub>), perfect prognosis-based multiple linear regression models are developed for 24-hr intensity change based on a combination of each of the aforementioned main predictors, together with previous 12-hr intensity change (PER) and 850- to 200-hPa vertical wind shear (SHRD). The last two predictors are widely used for intensity prediction and are always included as two additional predictors (Gao et al., 2016; Knaff et al., 2005; Kaplan et al., 2015). As listed in Table 1, four

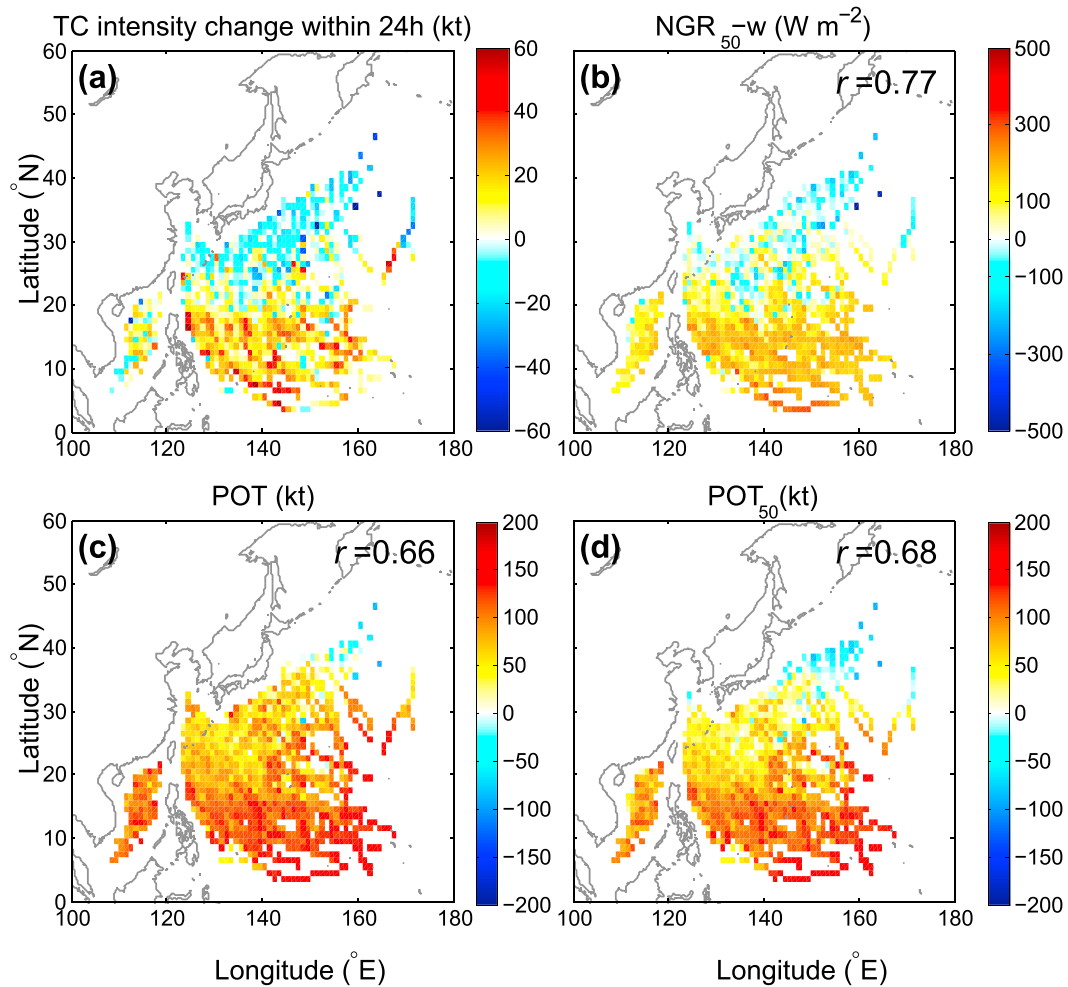


**Figure 2.** Composite (a) 6-hourly observed 24-hr tropical cyclone (TC) intensity change (kt), (b)  $NGR_{50-w}$  ( $W m^{-2}$ ), (c)  $POT$  (kt), and (d)  $POT_{50}$  (kt) in the  $1^\circ \times 1^\circ$  grid boxes during the period 2004–2016. The numbers in the top-right corner of (b)–(d) denote the correlation coefficient with (a).

sets of experiments are designed: (1) a run with the use of  $POT$  (hereafter referred to as EXP1); (2) a run with the use of  $DAT_{50}$ -based  $POT$  ( $POT_{50}$ ; hereafter referred to as EXP2); (3) a run with the use of  $DAT_{90}$ -based  $NGR-t$  ( $NGR_{90-t}$ ; hereafter referred to as EXP3); and (4) an experiment using  $NGR_{50-w}$  (hereafter referred to as EXP4). The four experiments are conducted to predict the 24-hr TC intensity change over the western North Pacific during 2004–2016. The SHRD is averaged within a 200-km radius after vortex removal.

**Table 1**  
*Experimental Designs for Investigating the Effect of Using the  $NGR_{50-w}$  on 24-hr TC Intensity Change*

Experiment	Predictor 1	Predictor 2	Predictor 3	Training period (2004–2014)		Test period (2015–2016)	
				MAE (kt)	$R^2$	MAE (kt)	$R^2$
EXP1	$POT$ (0.62)	PER (0.39)	SHRD (−0.36)	12.04	0.51	13.18	0.38
EXP2	$POT_{50}$ (0.63)			12.02	0.51	13.07	0.40
EXP3	$NGR_{90-t}$ (0.64)			12.26	0.48	12.40	0.43
EXP4	$NGR_{50-w}$ (0.69)			11.42	0.55	11.33	0.51

*Note.* The correlation coefficients between the predictors and 24-hr tropical cyclone (TC) intensity change during 2004–2016 are indicated in parentheses. The numbers in the subscript of  $POT$  and  $NGR$  refer to the depth of the ocean (in meters). The PER and SHRD indicate previous 12-hr intensity change and 850- to 200-hPa vertical wind shear. Mean absolute error (MAE) and  $R^2$  of 24-hr TC intensity changes for the four experiments are also compared during the training period (2004–2014) and test period (2015–2016).

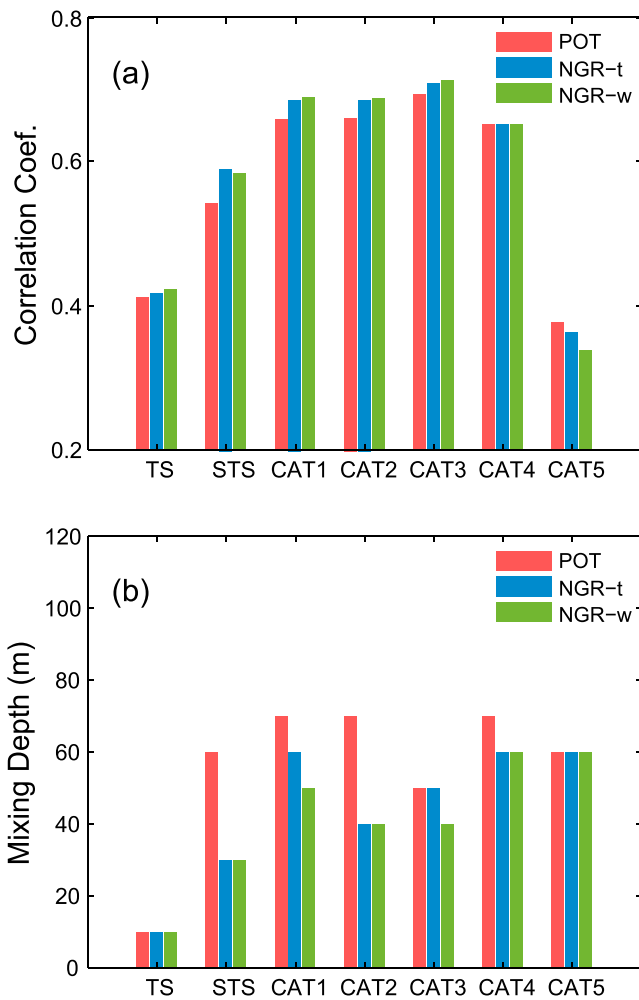


**Figure 3.** A comparison of the (a) maximum correlation coefficients from SST to  $DAT_{120}$  between 24-hr TC intensity change for three groups and (b) the mixing depth with the highest correlations by classifying TCs into seven intensity categories. TC = tropical cyclone; TS = tropical storm; STS = severe tropical storm; CAT1 = category 1; CAT2 = category 2; CAT3 = category 3; CAT4 = category 4; CAT5 = category 5; POT = the intensification potential; NGR-t = net energy gain rate using constant drag coefficient; NGR-w = same as NGR-t but for changing drag coefficient.

The performance of the four models in terms of mean absolute error (MAE) and  $R^2$  (coefficient of determination) is estimated from the training (2004–2014) and test (2015–2016) periods. For the training period, MAE and  $R^2$  were compared among the four models. Results show that EXP1 (using POT) is comparable to EXP2 (using  $POT_{50}$ ) and EXP3 (using  $NGR_{90-t}$ ), while EXP4 (using  $NGR_{50-w}$ ) shows the best performance (Table 1). EXP4 explains the highest  $R^2$  (55%) and has the lowest error (11.42 kt). For the independent period,  $NGR_{50-w}$  is, again, the best predictor with the lowest error and highest  $R^2$  among the four experiments (Table 1). Relative to EXP1, the 24-hr intensity change error decreases by up to 16% when the predictor  $NGR_{50-w}$  is used. These improvements in EXP4 for the training (test) period are statistically significant at the 5% (1%) level. Because  $NGR_{50-w}$  more realistically characterizes the interaction between TCs and the ocean using  $C_d$  depending on wind speed compared with  $NGR_{90-t}$  that uses a constant  $C_d$ , it serves as an effective predictor in improving prediction of TC intensity change at the shorter lead times (within 24 hr).

A comparison of the correlation coefficients between 24-hr TC intensity change and each of three groups (POT, NGR-t, and NGR-w) are also examined by classifying TCs into seven intensity categories according to initial maximum wind speed: tropical storm (34–47 kt), severe tropical storm (48–63 kt), category 1 (64–82 kt), category 2 (83–95 kt), category 3 (96–112 kt), category 4 (113–136 kt), and category 5 (above 137 kt). Figure 3a shows the maximum correlation coefficients from SST to  $DAT_{120}$  for 24-hr TC intensity changes for the three groups. Figure 3b displays the mixing depth with the highest correlations for the seven TC categories and all three groups. When storms are in the weakest stage (tropical storm), the highest correlations are almost identical for all three groups and occur at a very shallow mixing depth (~10 m) as shown in Figure 3 b. Intense TCs tend to have higher correlations with a deeper DAT for all groups and intensity categories. It also appears that the average mixing depth for NGR-w is ~50 m (Figure 3b). As expected, NGR-w exhibits a higher correlation with 24-hr TC intensity change than does POT for intensities below category 3 (Figure 3a), while NGR-w does not perform as well for the intensities above category 4. In fact, NGR-w has the lowest correlation coefficient among these three groups, especially for the intensities above category 5. This implies that constant  $C_d$  ( $2.0 \times 10^{-3}$ ) at extreme winds may not be optimal and one may parameterize  $C_d$  with an increasing or decreasing value or a constant but different value. The behavior of the air-sea exchange coefficient is controversial and still unclear at extreme wind speeds. We will return to this point later.

behavior of the air-sea exchange coefficient is controversial and still unclear at extreme wind speeds. We will return to this point later.

#### 4. A Comparison With Predictors From Other Recent Studies

This study also examined the effect of the use of TC-induced mixing depth varying with an individual TC state ( $T_{dy}$ ). This is motivated by recent studies (Balaguru et al., 2015, 2018) that suggest using  $T_{dy}$  yields a better prediction of TC intensification based on the National Hurricane Center's Statistical Hurricane Intensity Prediction Scheme. Following Balaguru et al. (2015), we calculate  $T_{dy}$  from the JTWC archive and HyCOM data for the same period and use the wind-dependent  $C_d$  as applied to NGR-w as described in section 2.2 ( $NGR_{T_{dy}}$ ). Our results show that  $NGR_{T_{dy}}$  has a lower correlation ( $r = 0.64$ ) with 24-hr TC intensity than has  $NGR_{50-w}$  ( $r = 0.69$ ), which is contrary to our expectations. However, the difference in correlations between Balaguru et al. (2015, 2018) and our study is not statistically significant.

A possible reason for this result could be the TC-wave-ocean coupling effect on momentum flux. Fan et al. (2009, 2010) showed that momentum flux is significantly reduced because of the strong dependence on the wave-induced processes near the ocean subsurface in a fully coupled wind-wave-ocean model. This reduction can be as large as 25% depending on the choice of the  $C_d$  parameterization. The parameterization of TC-induced mixing depth is therefore recommended to include the effect of wave-current interaction. Further studies are needed to find out more realistic drag coefficients when waves are incorporated in the parameterization scheme.

As mentioned previously, the behavior of  $C_d$  under very high wind speed conditions is uncertain although the  $NGR-w$  used here is wind dependent up to 120 kt. It might be possible for  $C_d$  to increase (Soloviev et al., 2014) or not change significantly at extreme wind speeds (Bell et al., 2012). It would be interesting to compare the results of  $NGR-w$  to an  $NGR$  using an increasing  $C_d$  above 120 kt ( $NGR-i$ ). A series of  $NGR-i$  is calculated (Soloviev et al., 2014), and we find that  $NGR-i$  also has a high correlation with 24-hr TC intensity change for all  $DAT$ . The maximum correlation coefficient of  $NGR-i$  is 0.68 at  $DAT_{50}$ , which is slightly lower than that of  $NGR_{50-w}$  ( $r = 0.69$ ). Therefore, in cases where  $C_d$  at very high wind speed is not known, a constant  $C_d$  may be used.

## 5. Discussion and Conclusion

A statistical-dynamical technique for TC intensity prediction combining statistical methodology with environmental predictors derived from numerical weather prediction system has been widely used over the last 25 years (DeMaria et al., 2005; DeMaria & Kaplan, 1994; DeMaria & Kaplan, 1999). The development of a new predictor, which has a high correlation with TC intensity, is directly connected to the improvement in prediction skill for a statistical-dynamical model.

$DAT$ -based  $POT$  shows higher correlation with 24-hr intensity change than does  $SST$ -based  $POT$ . However, for all the  $DAT$  (10–120 m) including  $SST$ ,  $NGR-w$  has higher correlations than has  $DAT$ -based  $POT$  (Figure 1), and improved 24-hr TC intensity prediction using  $NGR_{50-w}$  is achieved during both the training and independent periods (Table 1). The addition of a wind-dependent  $C_d$  to the dissipation term in  $NGR-w$  thus led to better prediction results for 24-hr intensity change. The findings in this study indicate that the best performance in predicting 24-hr TC intensity change was by the model at depth of 50 m ( $DAT_{50}$ ). This is somewhat different from the results of Price (2009) and Lin et al. (2013), who suggested that the best results for the ocean thermal field representing TC-ocean interaction are obtained from  $DAT_{100}$  and  $DAT_{80}$ , respectively. This difference may be attributed to the fact that all TC cases are used in this study, while the two previous studies only focused on stronger TCs.

To improve TC intensity change or rapid intensity change forecasts, this study suggests that  $POT$  predictors may be replaced by  $NGR_{50-w}$  because the latter more realistically represents the ocean contribution to 24-hr TC intensity change. In addition,  $NGR_{50-w}$  can be used to analyze the 24-hr TC intensity changes in the currently best performing intensity prediction models such as the Statistical Hurricane Intensity Prediction Scheme and Statistical-Dynamical Typhoon Intensity Prediction Scheme, because both models show little improvement at the shorter ranges (24–48 hr) (DeMaria et al., 2014).

Many studies have shown that TC intensity change is closely related to  $DAT$  and the parameterization of the air-sea exchange processes. We propose  $NGR$ , a new variant of an intensity change predictor related to Emanuel's (1988) MPI that uses the  $DAT$ , which includes information from TC-induced vertical mixing, and  $C_d$  dependent on wind speed (instead of a traditional constant  $C_d$ ). We show that the new index,  $NGR_{50-w}$ , improves the hindcasts of 24-hr TC intensity change and anticipate that this new index will contribute to improvements in real-time TC intensity forecasts, not only for the western North Pacific but also for other basins.

$NGR_{50-w}$  showed an overall positive bias (Figure S2) for a steady state condition. This implies that in addition to frictional dissipation, other environmental factors such as vertical wind shear might be considered with TC intensity changes in real-time forecasts. Lin et al. (2013) reported that  $OC\_PI$  is overestimated by about 10–20% because the atmospheric portion of the MPI equation is calculated under the assumption that the atmospheric profile does not have sufficient time to quickly adjust to the  $DAT$ . In this study,  $G$  is also calculated in the same manner, which results in positive bias of  $NGR_{50-w}$  for a steady state. In addition, it

should be noted that the correlation of  $NGR_{50-w}$  with intensity change is higher than the other predictors at shorter ranges (within 42 hr). Indeed, this result was statistically significant based on Fisher's  $z$  test, at the 5% test level from 6 to 36, 6 to 30, and 12 to 42 hr compared with the correlation of  $POT$ ,  $POT_{50}$ ,  $NGR_{90-t}$ , respectively, while after 48 hr the correlation coefficient does not reach 95% significance (Table S1). This is because the value of intensity-dependent  $NGR$  is calculated by the TC current intensity. Therefore, the TC intensity uncertainty increases with increasing forecast lead time and inconsistency between initial wind strength and TC intensities at the forecast lead times also increases.

We showed that the  $NGR$  index better estimates TC intensity change in the western North Pacific. Future work will apply the  $NGR$  index to other TC basins and verify that  $DAT_{50}$  shows the best performance in predicting 24-hr TC intensity change in this study with other years and other basins.

### Acknowledgments

This research is supported by "Development of typhoon analysis and forecast technology (1365003070)" of the National Typhoon Center/Korea Meteorological Administration and basic Science Research Program through the National Research Foundation of Korea (NRK) funded by the Ministry of Education (2017R1A2B2005019). The authors wish to thank May Izumi of the School of Ocean and Earth Science and Technology, University of Hawaii, and Luba Solonenko of Nova Southeastern University for their editorial assistance. TC data can be found in JTWC (<http://www.metoc.navy.mil/jtwc/jtwc.html>)? western-pacific), NCEP data at <https://nomads.nccd.noaa.gov/data/gfsan/>, and HyCOM NCODA data at <https://www.hycom.org/dataserver/>.

### References

- Balaguru, K., Foltz, G. R., Leung, L. R., D'Asaro, E., Emanuel, K. A., Liu, H., & Zedler, S. E. (2015). Dynamic potential intensity: An improved representation of the ocean's impact on tropical cyclones. *Geophysical Research Letters*, *42*, 6739–6746. <https://doi.org/10.1002/2015GL064822>
- Balaguru, K., Foltz, G. R., Leung, L. R., Hagos, S. M., & Judi, D. R. (2018). On the use of ocean dynamic temperature for hurricane intensity forecasting. *Weather and Forecasting*, *33*(2), 411–418. <https://doi.org/10.1175/WAF-D-17-0143.1>
- Bao, J.-W., Gopalakrishnan, S. G., Michelson, S. A., Marks, F. D., & Montgomery, M. T. (2012). Impact of physics representations in the HWRF model on simulated hurricane structure and wind–pressure relationships. *Monthly Weather Review*, *140*(10), 3278–3299. <https://doi.org/10.1175/MWR-D-11-00332.1>
- Bell, M. M., Montgomery, M. T., & Emanuel, K. A. (2012). Air-sea enthalpy and momentum exchange at major hurricane wind speeds observed during CBLAST. *Journal of the Atmospheric Sciences*, *69*(11), 3197–3222. <https://doi.org/10.1175/JAS-D-11-0276.1>
- Bister, M., & Emanuel, K. A. (1998). Dissipative heating and hurricane intensity. *Meteorology and Atmospheric Physics*, *52*, 233–240.
- Braun, S. A., & Tao, W.-K. (2000). Sensitivity of high-resolution simulations of Hurricane Bob (1991) to planetary boundary layer parameterizations. *Monthly Weather Review*, *128*(12), 3941–3961. [https://doi.org/10.1175/1520-0493\(2000\)129<3941:SOHRSO>2.0.CO;2](https://doi.org/10.1175/1520-0493(2000)129<3941:SOHRSO>2.0.CO;2)
- Chen, H., & Gopalakrishnan, S. (2014). A study on the asymmetric rapid intensification of Hurricane Earl (2010) using the HWRF system. *Proc. 31st Conference on Hurricanes and Tropical Meteorology*. San Diego, CA, 17D.5.
- Chen, P., Yu, H., & Chan, J. C. L. (2011). A western North Pacific tropical cyclone intensity prediction scheme. *Acta Meteorologica Sinica*, *25*(5), 611–624. <https://doi.org/10.1007/s13351-011-0506-9>
- Chu, P.-S., & Zhao, X. (2007). A Bayesian regression approach for predicting tropical cyclone activity over the central North Pacific. *Journal of Climate*, *20*(15), 4002–4013. <https://doi.org/10.1175/JCLI4214.1>
- DeMaria, M., DeMaria, R. T., Knaff, J. A., & Molenaar, D. (2012). Tropical cyclone lightning and rapid intensity change. *Monthly Weather Review*, *140*(6), 1828–1842. <https://doi.org/10.1175/MWR-D-11-00236.1>
- DeMaria, M., & Kaplan, J. (1994). A Statistical Hurricane Intensity Prediction Scheme (SHIPS) for the Atlantic basin. *Weather and Forecasting*, *9*(2), 209–220. [https://doi.org/10.1175/1520-0434\(1994\)009<0209:ASHIPS>2.0.CO;2](https://doi.org/10.1175/1520-0434(1994)009<0209:ASHIPS>2.0.CO;2)
- DeMaria, M., & Kaplan, J. (1999). An updated Statistical Hurricane Intensity Prediction Scheme (SHIPS) for the Atlantic and eastern North Pacific basins. *Weather and Forecasting*, *14*(3), 326–337. [https://doi.org/10.1175/1520-0434\(1999\)014<0326:AUSHIP>2.0.CO;2](https://doi.org/10.1175/1520-0434(1999)014<0326:AUSHIP>2.0.CO;2)
- DeMaria, M., Mainelli, M., Shay, L. K., Knaff, J. A., & Kaplan, J. (2005). Further improvements to the Statistical Hurricane Intensity Prediction Scheme (SHIPS). *Weather and Forecasting*, *20*(4), 531–543. <https://doi.org/10.1175/WAF862.1>
- DeMaria, M., Sampson, C. R., Knaff, J. A., & Musgrave, K. D. (2014). Is tropical cyclone intensity guidance improving? *Bulletin of the American Meteorological Society*, *95*(3), 387–398. <https://doi.org/10.1175/BAMS-D-12-00240.1>
- Donelan, M. A., Haus, B. K., Reul, N., Plant, W. J., Stiassnia, M., Graber, H. C., et al. (2004). On the limiting aerodynamic roughness of the ocean in very strong winds. *Geophysical Research Letters*, *31*, L18306. <https://doi.org/10.1029/2004GL019460>
- Elsberry, R. L., Chen, L., Davidson, J., Rogers, R., Wang, Y., & Wu, L. (2013). Advances in understanding and forecasting rapidly changing phenomena in tropical cyclones. *Tropical Cyclone Research and Review*, *2*, 13–24.
- Emanuel, K. A. (1986). An air-sea interaction theory for tropical cyclones. Part I: Steady-state maintenance. *Journal of the Atmospheric Sciences*, *43*(6), 585–605. [https://doi.org/10.1175/1520-0469\(1986\)043<0585:AASITF>2.0.CO;2](https://doi.org/10.1175/1520-0469(1986)043<0585:AASITF>2.0.CO;2)
- Emanuel, K. A. (1988). The maximum intensity of hurricanes. *Journal of the Atmospheric Sciences*, *45*(7), 1143–1155. [https://doi.org/10.1175/1520-0469\(1988\)045,1143:TMIOH.2.0.CO;2](https://doi.org/10.1175/1520-0469(1988)045,1143:TMIOH.2.0.CO;2)
- Emanuel, K. A. (1995). Sensitivity of tropical cyclones to surface exchange coefficients and a revised steady-state model incorporating eye dynamics. *Journal of the Atmospheric Sciences*, *52*(22), 3969–3976. [https://doi.org/10.1175/1520-0469\(1995\)052<3969:SOTCTS>2.0.CO;2](https://doi.org/10.1175/1520-0469(1995)052<3969:SOTCTS>2.0.CO;2)
- Emanuel, K. A. (2003). A similarity hypothesis for air–sea exchange at extreme wind speeds. *Journal of the Atmospheric Sciences*, *60*(11), 1420–1428. [https://doi.org/10.1175/1520-0469\(2003\)060<1420:ASHFAE>2.0.CO;2](https://doi.org/10.1175/1520-0469(2003)060<1420:ASHFAE>2.0.CO;2)
- Emanuel, K. A., DesAutels, C., Holloway, C., & Korty, R. (2004). Environmental control of tropical cyclone intensity. *Journal of the Atmospheric Sciences*, *61*(7), 843–858. [https://doi.org/10.1175/1520-0469\(2004\)061<0843:ECOTCI>2.0.CO;2](https://doi.org/10.1175/1520-0469(2004)061<0843:ECOTCI>2.0.CO;2)
- Fan, Y., Ginis, I., & Hara, T. (2009). The effect of wind-wave-current interaction on air-sea momentum fluxes and ocean response in tropical cyclones. *Journal of Physical Oceanography*, *39*(4), 1019–1034. <https://doi.org/10.1175/2008JPO4066.1>
- Fan, Y., Ginis, I., & Hara, T. (2010). Momentum flux budget across the air-sea interface under uniform and tropical cyclone winds. *Journal of Physical Oceanography*, *40*(10), 2221–2242. <https://doi.org/10.1175/2010JPO4299.1>
- Gall, R., Franklin, J., Marks, F., Rappaport, E. N., & Toepfer, F. (2013). The hurricane forecast improvement project. *Bulletin of the American Meteorological Society*, *94*(3), 329–343. <https://doi.org/10.1175/BAMS-D-12-00071.1>
- Gao, S., Zhang, W., Liu, J., Lin, I.-I., Chiu, L. S., & Cao, K. (2016). Improvements in typhoon intensity change classification by incorporating an ocean coupling potential intensity index into decision trees. *Weather and Forecasting*, *31*(1), 95–106. <https://doi.org/10.1175/WAF-D-15-0062.1>
- Goni, G., DeMaria, M., Knaff, J., Sampson, C., Ginis, I., Bringas, F., et al. (2009). Applications of satellite-derived ocean measurements to tropical cyclone intensity forecasting. *Oceanography*, *22*(3), 190–197. <https://doi.org/10.5670/oceanog.2009.78>

- Green, B. W., & Zhang, E. (2013). Impacts of air–sea flux parameterizations on the intensity and structure of tropical cyclones. *Monthly Weather Review*, *141*(7), 2308–2324. <https://doi.org/10.1175/MWR-D-12-00274.1>
- Holland, G. J. (1997). The maximum potential intensity of tropical cyclones. *Journal of the Atmospheric Sciences*, *54*(21), 2519–2541. [https://doi.org/10.1175/1520-0469\(1997\)054<2519:TMPIOT>2.0.CO;2](https://doi.org/10.1175/1520-0469(1997)054<2519:TMPIOT>2.0.CO;2)
- Jarosoz, E., Mitchell, D. A., Wang, D. W., & Teague, W. J. (2007). Bottom-up determination of air–sea momentum exchange under a major tropical cyclone. *Science*, *315*(5819), 1707–1709. <https://doi.org/10.1126/science.1136466>
- Jenkins, A. D. (2002). Do strong winds blow waves flat? In B. L. Edge & J. M. Hemsley (Eds.), *Ocean Wave Measurement and Analysis: Proceedings of the Fourth International Symposium, WAVES 2001: September 2–6, 2001, San Francisco, California* (pp. 494–500). Reston, Va: Am. Soc. of Civ. Eng.
- Kaplan, J., Rozoff, C. M., DeMaria, M., Sampson, C. R., Kossin, J. P., Velden, C. S., et al. (2015). Evaluating environmental impacts on tropical cyclone rapid intensification predictability utilizing statistical models. *Weather and Forecasting*, *30*(5), 1374–1396. <https://doi.org/10.1175/WAF-D-15-0032.1>
- Kaplan, J., DeMaria, M., & Knaff, J. A. (2010). A revised tropical cyclone rapid intensification index for the Atlantic and eastern North Pacific basins. *Weather and Forecasting*, *25*(1), 220–241. <https://doi.org/10.1175/2009WAF2222280.1>
- Kim, S.-H., Moon, I.-J., & Chu, P.-S. (2018). Statistical-dynamic typhoon intensity predictions in the western North Pacific using track pattern clustering and ocean coupling predictors. *Weather and Forecasting*, *33*(1), 347–365. <https://doi.org/10.1175/WAF-D-17-0082.1>
- Knaff, J. A., Sampson, C. R., & DeMaria, M. (2005). An operational Statistical Typhoon Intensity Prediction Scheme for the western North Pacific. *Weather and Forecasting*, *20*(4), 688–699. <https://doi.org/10.1175/WAF863.1>
- Lin, I.-I., Black, P., Price, J. F., Yang, C.-Y., Chen, S. S., Lien, C.-C., et al. (2013). An ocean coupling potential intensity index for tropical cyclones. *Geophysical Research Letters*, *40*, 1878–1882. <https://doi.org/10.1002/grl.50091>
- Lin, I.-I., Chen, C.-H., Pun, I.-F., Liu, W. T., & Wu, C.-C. (2009). Warm ocean anomaly, air sea fluxes, and the rapid intensification of tropical cyclone Nargis (2008). *Geophysical Research Letters*, *36*, L03817. <https://doi.org/10.1029/2008GL03581>
- Lin, I.-I., Wu, C. C., Pun, I. F., & Ko, D. S. (2008). Upper-ocean thermal structure and the western North Pacific category-5 typhoons. Part I: Ocean features and category-5 typhoon's intensification. *Monthly Weather Review*, *136*(9), 3288–3306. <https://doi.org/10.1175/2008MWR2277.1>
- Lin, N., Jing, R., Wang, Y., Yonekura, E., Fan, J., & Xue, L. (2017). A statistical investigation of the dependence of tropical cyclone intensity change on the surrounding environment. *Monthly Weather Review*, *145*(7), 2813–2831. <https://doi.org/10.1175/MWR-D-16-0368.1>
- Mei, W., & Xie, S.-P. (2016). Intensification of landfalling typhoons over the northwest Pacific since the late 1970s. *Nature Geoscience*, *9*(10), 753–757. <https://doi.org/10.1038/ngeo2792>
- Montgomery, M. T., Smith, R. K., & Nguyen, S. V. (2010). Sensitivity of tropical-cyclone models to the surface drag coefficient. *Quarterly Journal of the Royal Meteorological Society*, *136*(653), 1945–1953. <https://doi.org/10.1002/qj.702>
- Moon, I.-J., Ginis, I., Hara, T., & Thomas, B. (2007). A physics-based parameterization of air–sea momentum flux at high wind speeds and its impact on hurricane intensity predictions. *Monthly Weather Review*, *135*(8), 2869–2878. <https://doi.org/10.1175/MWR3432.1>
- Nolan, D. S., Stern, D. P., & Zhang, J. A. (2009). Evaluation of planetary boundary layer parameterizations in tropical cyclones by comparison of in situ observations and high-resolution simulations of Hurricane Isabel (2003). Part II: Inner-core boundary layer and eye-wall structure. *Monthly Weather Review*, *137*, 3675–3698.
- Nolan, D. S., Zhang, J. A., & Stern, D. P. (2009). Evaluation of planetary boundary layer parameterizations in tropical cyclones by comparison of in situ observations and high-resolution simulations of Hurricane Isabel (2003). Part I: Initialization, maximum winds, and the outer-core boundary layer. *Monthly Weather Review*, *137*(11), 3651–3674. <https://doi.org/10.1175/2009MWR2785.1>
- Ooyama, K. (1969). Numerical simulation of the life cycle of tropical cyclones. *Journal of the Atmospheric Sciences*, *26*(1), 3–40. [https://doi.org/10.1175/1520-0469\(1969\)026<0003:NSOTLC>2.0.CO;2](https://doi.org/10.1175/1520-0469(1969)026<0003:NSOTLC>2.0.CO;2)
- Powell, M. D., Vickery, P. J., & Reinhold, T. A. (2003). Reduced drag coefficient for high wind speeds in tropical cyclones. *Nature*, *422*(6929), 279–283. <https://doi.org/10.1038/nature01481>
- Price, J. F. (2009). Metrics of hurricane–ocean interaction: Vertically-integrated or vertically-averaged ocean temperature? *Ocean Science*, *5*(3), 351–368. <https://doi.org/10.5194/os-5-351-2009>
- Pun, I. F., Lin, I.-I., Wu, C. R., Ko, D. S., & Liu, W. T. (2007). Validation and application of altimetry-derived upper ocean thermal structure in the Western North Pacific Ocean for typhoon intensity forecast. *IEEE Transactions on Geoscience and Remote Sensing*, *45*(6), 1616–1630. <https://doi.org/10.1109/TGRS.2007.895950>
- Quenouille, M. A. (1952). *Associated measurements* (p. 242). London: Butterworths.
- Rappaport, E. N., Jiing, J. G., Landsea, C. W., Murillo, S. T., & Franklin, J. L. (2012). The Joint Hurricane Testbed—Its first decade of tropical cyclone research-to-operations activities revisited. *Bulletin of the American Meteorological Society*, *93*(3), 371–380. <https://doi.org/10.1175/BAMS-D-11-00037.1>
- Rotunno, R., & Emanuel, K. A. (1987). An air–sea interaction theory for tropical cyclones. Part II: Evolutionary study using a nonhydrostatic axisymmetric numerical model. *Journal of the Atmospheric Sciences*, *44*(3), 542–561. [https://doi.org/10.1175/1520-0469\(1987\)044<0542:AAITFT>2.0.CO;2](https://doi.org/10.1175/1520-0469(1987)044<0542:AAITFT>2.0.CO;2)
- Rozoff, C. M., & Kossin, J. P. (2011). New probabilistic forecast models for the prediction of tropical cyclone rapid intensification. *Weather and Forecasting*, *26*(5), 677–689. <https://doi.org/10.1175/WAF-D-10-05059.1>
- Shay, L. K., Goni, G. J., & Black, P. G. (2000). Effects of a warm oceanic feature on Hurricane Opal. *Monthly Weather Review*, *128*(5), 1366–1383. [https://doi.org/10.1175/1520-0493\(2000\)128<1366:EOAWOF>2.0.CO;2](https://doi.org/10.1175/1520-0493(2000)128<1366:EOAWOF>2.0.CO;2)
- Soloviev, A. V., Lukas, R., Donelan, M. A., Haus, B. K., & Ginis, I. (2014). The air–sea interface and surface stress under tropical cyclones. *Scientific Reports*, *4*(1), 5306. <https://doi.org/10.1038/srep05306>
- Takagaki, N., Komori, S., Suzuki, N., Iwano, K., Kuramoto, T., Shimada, S., et al. (2012). Strong correlation between the drag coefficient and the shape of the wind sea spectrum over a broad range of wind speeds. *Geophysical Research Letters*, *39*, L23604. <https://doi.org/10.1029/2012GL053988>
- Tallarpragada, V., & Kieu, C. (2014). Real-time forecasts of typhoon rapid intensification in the north Western Pacific basin with the NCEP operational HWRF model. *Tropical Cyclone Research and Review*, *3*(2), 63–76.
- Wada, A., & Usui, N. (2007). Importance of tropical cyclone heat potential for tropical cyclone intensity and intensification in the Western North Pacific. *Journal of Oceanography*, *63*(3), 427–447. <https://doi.org/10.1007/s10872-007-0039-0>
- Wilks, D. S. (2011). *Statistical methods in the atmospheric sciences* (3rd ed., p. 676). Oxford; Waltham, MA: Academic Press.